Viewing Geometry of AVHRR Image Composites Derived Using Multiple Criteria

David M. Stoms, Michael J. Bueno, and Frank W. Davis

Abstract

The U.S. Geological Survey currently generates composites of AVHRR imagery based on a single objective—maximizing the Normalized Difference Vegetation Index (NDVI)—as a means of reducing cloud contamination. Our research supports the findings of others that, in some cases, NDVI is maximized at the expense of optimal viewing geometry; that is, satellite zenith angles are often further off-nadir than necessary to ensure cloud-free viewing. We explore various compositing methods by systematically varying weights on NDVI, satellite zenith angle, and maximum apparent temperature. A test composite of California from September 1990 appears to be superior to the maximum NDVI and maximum apparent temperature composites in several respects. First, the satellite zenith angle distribution is more closely clustered about nadir, which minimizes atmospheric path length, spatial distortion, and bidirectional reflectance effects. Second, neighboring pixels are more frequently selected with similar viewing geometry and atmospheric conditions.

Introduction

Compositing is a strategy for removing cloud contamination and atmospheric effects from a series of images over a discrete period of time. The U.S. Geological Survey's (USGS) EROS Data Center (EDC) has an operational program for developing 1-km resolution Advanced Very High Resolution Radiometer (AVHRR) data sets over the conterminous U.S. (Eidenshink, 1992). The conterminous AVHRR time series data are produced using the maximum value compositing (MVC) technique based on the Normalized Difference Vegetation Index (NDVI) (Holben, 1986). The highest vegetation index value derived from daily georeferenced images is selected for each pixel location in a 14-day period. Clouds and their shadows have low NDVI values relative to the true index value of vegetated surfaces. In theory, the maximum value technique leads to the selection of the greenest and, therefore, least cloud-contaminated data value. Based on this method, a biweekly composite data set is created that includes the five satellite data channels, the vegetation index, viewing geometry, and date of pixel observation. This time series of AVHRR data is distributed by EDC on CD-ROM for the years 1989 through 1993 (Eidenshink, 1992). NDVI values, which range from -1 to $+1$, are rescaled to 8-bit data between 0 and 200 in the EDC time series data. The compositing strategy currently being applied to create a global 1-km dataset, commencing with 1992 imagery, is similar except that the compositing period is only 10 days and a constraint to eliminate satellite zenith angles greater than 42° was added (Eidenshink and Faundeen, 1994).

When the MVC algorithm was originally proposed, it was argued that the method would preferentially select near-nadir views over larger scan angles (Holben, 1986). The work that led to that recommendation was based on a model using an assumption of Lambertian reflectance from Earth surfaces. Numerous studies have found that off-nadir viewing can produce greater NDVI values than at nadir viewing angles. Deering and Eck (1987) found the highest NDVI in the forward-scatter direction for grass and soybean cover, in large part caused by greater shadowing from the plant canopy in this direction. The scan direction of the afternoon satellites used for compositing also is near the principal plane of the sun in the northern hemisphere, which can accentuate the amount of shadowing from the canopy even further (Goward *et al.*, 1991). Yang *et al.* (1996) observed a similar forward-scatter bias in the North American portion of the global 1-km dataset averaged over one year, but not for the South American composites. Possibly, the relationship with the principal plane of the sun is responsible for this geographic difference. Gutman (1991) showed strong forward-scatter bias in a 10-day NDVI composite over the Great Plains using a 40-km resolution dataset. Cihlar *et al.* (1994) observed that the MVC algorithm preferentially selected forescattering views over nadir for a variety of cover types in central Canada. They attributed this to a higher transmittance of near infrared radiation through the canopy compared with red radiation. On the east coast of the United States, results have been contrary (Allen *et al.*, 1994; Moody and Strahler, 1994). Satellite zenith angle distribution was biased towards backscatter views. Moody and Strahler (1994) suggested that this bias was caused by two factors: that westward-looking or forward-scatter views may not have been available in the dataset and that scanning in New England was not near the principal plane of the sun. The first factor was presumably a result of the AVHRR data being acquired at the EDC in Sioux Falls, South Dakota, and consequently limiting the number of dates, and angles, available. The relationship of viewing to the principal plane of the sun would reduce the main anisotropic effects from the atmosphere and the surface. Certainly the combination of off-nadir bias in compositing and regional variations in effects would make it more difficult to interpret NDVI derived from AVHRR composites over the conterminous U. S. or globally. Biophysical modelers would encounter an added level of uncertainty when using these composites as inputs.

Off-nadir viewing causes several potential problems for interpreting NDVI. For off-nadir views, the Instantaneous Field of View (IFOV) integrates surface leaving radiance from a larger footprint on the ground than the output pixel area, and it overlaps the IFOV of neighboring pixels. Furthermore, the scattering properties of the atmosphere are directional,

Department of Geography and Institute for Computational Earth System Science, University of California, Santa Barbara, CA 93106-4060 (stoms@geog.ucsb.edu).

Photogrammetric Engineering & Remote Sensing, Vol. 63, No. 6, June 1997, pp. 681–689.

0099-1112/97/6306-681$3.00/0

meaning that views towards the sun will be affected by quite different scattering than views away from the sun at the same viewing angle. Most Earth surface materials also exhibit an anisotropic property, further distorting the reflectance observed at the satellite from the true values at ground level. Therefore, it is important to more fully understand the characteristics of the NDVI time series data from EDC with respect to viewing geometry. Concurrently, the need to explore alternative compositing strategies has been widely recognized (Viovy *et al.*, 1992; Cihlar *et al.*, 1994; Eidenshink and Faundeen, 1994; Townshend *et al.*, 1994).

We undertook an analysis of the 1990 AVHRR time series to examine its viewing characteristics on the west coast of the United States. We also experimented with alternative compositing algorithms to reduce the potential satellite zenith angle bias. The objectives of this paper are (1) to quantify the viewing geometry of the 1990 composites derived by the maximum NDVI value algorithm and interpret these findings in relation to land cover for California, and (2) to evaluate alternative algorithms that systematically vary the importance of three criteria in the compositing process. The distributions of satellite zenith angles from the alternatives are compared. Three alternatives are compared: MVC, maximum apparent temperature (MaT) (Cihlar *et al.*, 1994), and one that includes both maximum apparent temperature and satellite zenith angle criteria. We refer to this multiple objective compositing algorithm by the acronym MOC.

Background

The EDC NDVI time series has been used for a wide variety of applications, including land-cover mapping and characterization (Loveland *et al.*, 1991; Kremer and Running, 1993; Paruelo and Lauenroth, 1995), crop assessments (Wade *et al.*, 1994), fire monitoring (Kasischke *et al.*, 1993), biodiversity assessment (Walker *et al.*, 1992), and interannual variation in plant phenology (Reed *et al.*, 1994). For many if not all of these applications at regional and larger scales, it is essential that data be compiled consistently so that NDVI has a constant relationship with biophysical parameters.

The AVHRR sensor achieves its daily global coverage by means of scan sweeps to over 55 degrees off-nadir, producing a look angle of 68 degrees relative to the Earth's surface. Off-nadir viewing causes at least three potential problems for computing and interpreting NDVI: variations in spatial resolution, variations in atmospheric attenuation associated with changes in path length, and variations in bidirectional reflectance effects (Goward *et al.*, 1991). Whereas a pixel at nadir has a spatial resolution of 1.1 km, at the extreme angle the effective resolution is 2.4 km by 6.5 km. Adjacent pixels of off-nadir observations also have significant overlap. Goward *et al.* (1991) calculate that the IFOV becomes significantly distorted beyond off-nadir zenith angles of 25 degrees. The information for each 1.21-km^2 pixel in the geometrically corrected output is derived from an actual area of up to 16 km^2 on the ground.

All satellite remote sensing is subject to the atmospheric attenuation of surface-leaving radiance. Off-nadir viewing increases this effect by lengthening the path that the reflected energy traverses. Furthermore, the scattering properties of the atmosphere are directional, meaning that views towards the sun will be affected differently than views away from the sun at the same angle. Aerosol scattering is more pronounced in the red channel of AVHRR (Channel 1) than in the near infrared (Channel 2), and is strongest in the backscatter direction (eastward looking on the afternoon satellite passes) (Deering and Eck, 1987; Holben *et al.*, 1986).

Most Earth-surface materials also exhibit anisotropic reflectance characteristics, further modulating the reflectance observed at the satellite relative to the true value at ground level. Holben *et al.* (1986), for instance, showed that NDVI of grasses tends to be lowest at extreme scan angles in the backscatter direction and highest in the forward scatter direction. The combined effect then, for equivalent atmospheric and surface conditions, is that NDVI will tend to be lower in the backscatter direction, and will be highest in the forescattering direction, or westward looking, than in either the eastward or nadir views (Goward *et al.*, 1991).

The potential impacts of viewing angle on NDVI and on cover-type classification led us to review the remote sensing literature for alternative compositing algorithms that might guarantee close-to-nadir composites. In a comparison of five algorithms, Cihlar *et al.* (1994) found that maximum apparent temperature produced composites which were consistently closest to nadir for crops and relatively close for forest types in Canada. Also, neighboring pixels were more often selected from the same scene, reducing artificial texture in the NDVI composite. Equally important, maximum apparent temperature produced NDVI values closest to a reference image. Another advantage of this method is that it uses data within the dataset rather than depending on ancillary meteorological or environmental data which may be incomplete.

The maximum-apparent-temperature algorithm is based on the observation that clouds decrease the apparent surface temperature. Off-nadir pixels would also tend to be *excluded* if other choices were available because the increased path length further attenuates the emitted thermal signal. It could be subject to rejection of nadir views if surface conditions affect apparent temperature more than the atmospheric effects do, e.g., rainfall over bare soil. The algorithm used by Cihlar *et al.* (1994) is based on AVHRR Channel 4, in the 10.3 to 11.3 micrometre range. As a second choice, they also recommend a two-step procedure using the maximum NDVI followed by a minimum scan angle criterion applied to all pixels within 15 percent of maximum NDVI in that period.

Methods

Viewing Geometry of the 1990 Time Series Composites

For the state of California, the satellite zenith angle files for the 19 composites of the 1990 time series were obtained from the CD-ROM (USGS, 1991) and averaged for every pixel. From visual examination of this derived image, there appeared to be a probable relationship between viewing geometry of the NDVI data and both vegetation and topographic features. In order to quantify these apparent relationships, the CALVEG map of plant series (Matyas and Parker, 1980) was recoded to general types, i.e., subformations, and gridded to the same resolution as the AVHRR-based data. An identical 10 percent random sample was taken from the NDVI images and the vegetation map for statistical analysis in S-PLUS (Statistical Sciences, Inc., 1991). The size of the sample (greater than 40,000 samples) was large enough that all types would be proportionally represented. Therefore, stratifying the sampling by vegetation types was deemed unnecessary. Data were analyzed by examining the frequency histograms of NDVI and viewing geometry and by creating boxplots of angles by land-cover class.

Alternative Compositing Strategies

To evaluate alternative compositing algorithms, we obtained the daily georectified AVHRR data from EDC. The California study area was windowed from reflectance Bands 1 and 2, thermal Band 4, and the satellite zenith angle files for each daily image. The composite period of 14 September to 27 September 1990 was selected for several reasons. It is late in the summer dry season in California's Mediterranean climate, and the contrast between many vegetation types is high then. The landscape is not saturated with peak green-

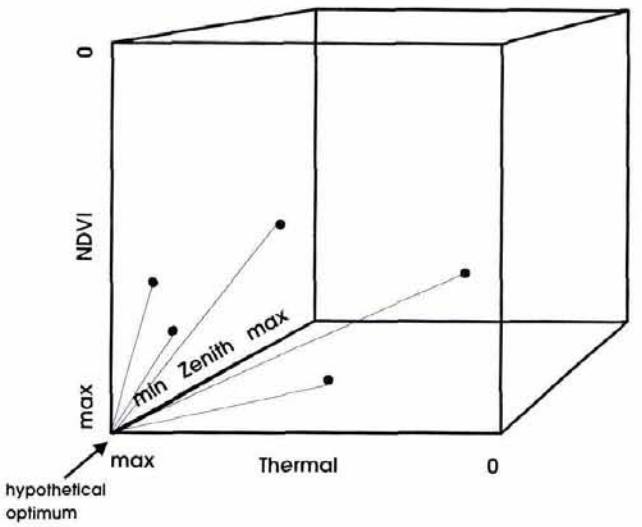

Figure 1. Diagram of a hypothetical AVHRR dataset showing the distribution of pixel values in the dimensions of thermal DN, Normalized Difference Vegetation Index (NDVI), and satellite zenith angle. The hypothetical optimum at the origin of the measurement space is based on the optimal value of each variable for the pixel from all the image dates in the composite period. Thus, the optimum is recomputed for each pixel in each time period.

ness of the annual grasslands or agricultural crops. This contrast is valuable, given our interest in AVHRR data for land-cover mapping and monitoring. It is also late enough in the year that most snow cover is gone from the higher peaks. Most of the daily images contained some cloud cover, most frequently over the northwest corner, the Sierra Nevada range, and the southern quarter of the study area. Therefore, the basic compositing objective of cloud removal could be reasonably tested.

There are three criteria to consider for the selection of the best pixels for a given composite period: pixels chosen would ideally have the minimum satellite zenith angle, the maximum vegetation index values, and the maximum apparent temperature values of all candidate pixels for a single pixel on the ground. The advantages of viewing geometry and maximum NDVI criteria have been discussed above. Maximum apparent temperature is also a potentially useful criterion because both clouds and off-nadir viewing tend to decrease the apparent surface temperature. Furthermore, all three variables are provided within the daily image datasets routinely processed by EDC (Cihlar *et al.*, 1994). No independent data with comprehensive coverage are required.

In order to test the viability of selecting the "best" pixel in a time series for a given geopixel location with high vegetation index, high apparent temperature, and low satellite zenith angle concurrently, a multiple-objective procedure was developed. The criteria represent different kinds of variables, and there is no theoretical basis for assigning them weights. We chose therefore to take an exploratory approach in which we could vary the weights systematically and, in an empirical manner, identify a suitable set of weights for this particular example. It is likely that the hypothetically optimal pixel does not exist, however, but finding the pixel closest to this hypothetically optimal case allows the flexibility to decide between pixels with similar values of a single criterion at the same pixel location. In order to find the "best" pixel considering all three criteria, imagine a three-dimensional scatterplot with axes for vegetation index, apparent temperature, and satellite zenith angle, and with the hypothetical optimum pixel at the origin (shown conceptually in Figure 1). The multi-dimensional Euclidean distance of the pixel from each image in the compositing period is calculated, and the one with the shortest distance to the hypothetical optimum is chosen. The value of the hypothetically optimal pixel is recomputed for each spatial location based on the range of values for that pixel across the compositing period. The three axes, of course, are in different units and it is necessary to scale each axis independently. Thermal and NDVI variables were each tested at weights of 0.0, 0.5, and 1.0 while satellite zenith angle was varied from 0.0, 0.1, and 0.2. The MVC algorithm corresponds to weights of 1.0 for maximum NDVI and zeros for the other objectives. Similarly, the MaT algorithm only has a weight assigned to the maximum apparent temperature criterion.

The first step was to select a set of weights to represent the MOC composite. The various weighted 14-day composites of AVHRR Band 1 for period #15 in September, 1990, were compared for a small window within California corresponding to the footprint of three contiguous 1990 Thematic Mapper (TM) scenes (TM paths/rows 42/34 and 42/35—25 August; and 41/35—3 September). The mosaic of TM scenes was chosen as the reference image for comparison because they are cloud-free, have an almost nadir viewing angle, and were acquired within three weeks from the start of the AVHRR composite period. The three TM scenes were mosaicked together, and the mosaic was resampled to a 1-km pixel size using a mean filter operation which assigned the mean value of Band 3 in a moving window to an output image. Because the red and near infrared wavelengths for the two sensors do not exactly correspond, the comparisons were made using correlations for the visible channels instead of NDVI. In particular, the wider bandpass of the AVHRR near infrared band is more sensitive to water vapor than its narrower counterpart in TM (Goward *et al.*, 1991). The correlation between the resampled red TM Band 3 and the visible AVHRR Band 1 was recorded for each combination of weights in order to provide insight into which weights produced TM-quality composites. Again, the correlation was used rather than actual values because the spectral bandwidth of TM and AVHRR are not identical. The comparison to TM was not considered definitive in the selection of the best compositing algorithm but, instead, it provided insight into which variables and weight combinations are most important.

Correlation values between the TM and AVHRR visible channels varied from 0.433 to 0.851 for the different weight combinations (Table 1). Combinations with a positive thermal weight were always higher than those without. The same was not true for NDVI, however, as the correlations were virtually the same for all NDVI weights. The highest correlation overall was for a weight of 1.0 for maximum apparent temperature with no weight given to angle or NDVI. In

TABLE 1. CORRELATIONS BETWEEN COMPOSITED AVHRR CHANNEL 1 DATA WITH TM CHANNEL 3. THE AVHRR COMPOSITES VARY BY THE WEIGHTS GIVEN TO THE THERMAL (MAXIMUM APPARENT TEMPERATURE), NDVI, AND SATELLITE ZENITH ANGLE CRITERIA.

		NDVI Wt. 0.0			0.5			1.0		
		Angle wt. 0.0	0.1	0.2	0.0	0.1	0.2	0.0	0.1	0.2
Thermal wt.	0.0	—	0.433	0.433	—	0.689	0.643	0.778	0.743	0.696
	0.5	—	0.838	0.831	0.841	0.841	0.839	0.837	0.840	0.839
	1.0	0.851	0.844	0.844	0.844	0.844	0.842	0.840	0.841	0.841

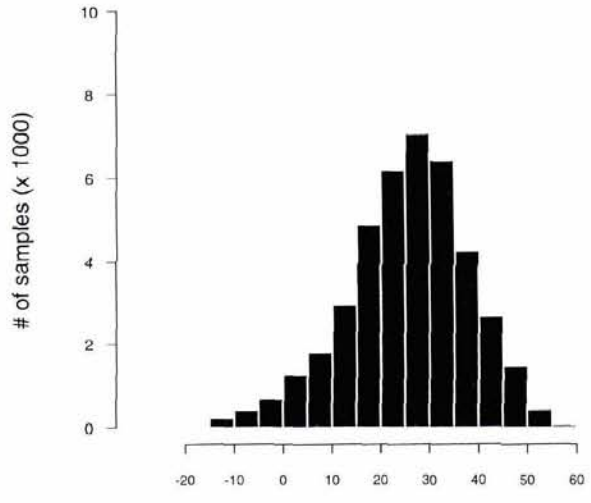

Figure 2. Histogram of the frequency of satellite zenith angles averaged over the 19 biweekly composites. Nadir is at 0°, backscatter (eastward) views are negative numbers, and forescatter (westward) views are positive.

fact, correlations were consistently between 0.83 and 0.85 if the apparent temperature was positively weighted. Generally, adding an angle weight caused the correlation to decrease slightly for constant weights for the other two criteria, although the lowest correlation was still 0.841. The correlation for NDVI with a weight of 1 and no weight for thermal or angle was 0.778. Increasing the weight for the thermal criterion while maintaining the NDVI weight produced a small increase in correlation, up to 0.840 for equal weighting of NDVI and thermal.

These results indicate that a high quality composite for the visible channel can be achieved using a straight maximum-apparent-temperature (MAT) or a maximum-value (MVC) algorithm. The outcome is sensitive to the angle weight, and a small angle weight is preferable to a larger weight. This makes sense as the range of angle values is much smaller (0 to 64) as compared to the rescaled DN values of NDVI (0 to 200) or the thermal band (0 to 255). The highest correlation values using a maximum-apparent-temperature algorithm coupled with the knowledge of the sensitivity of the angle weights prompted us to make some composites with very small angle weights (< 0.2) and a thermal weight of 1. The images produced by the weight combinations with the highest correlations were visually inspected. The histograms of satellite zenith angle were also inspected for consistency in selecting lower angles. For these data, the best composite was produced using a thermal weight of 1, an angle weight of 0.1, and an NDVI weight of 0. These weights were applied for the MOC alternative for all subsequent analyses. We eliminated the composite based on positive weighting of all three criteria because it made no improvement in viewing angle and, in fact, did a poorer job separating clouds from water than the final MOC weights that ignored NDVI.

The three compositing algorithms (MVC, MAT, and MOC) were evaluated using three methods. First, the distribution of satellite zenith angles were compared. If the differences are minimal, either there was little choice among daily images because of cloud contamination in the near-nadir data or else all daily images were similar despite differences in viewing geometry. The second evaluation compared the distribution of satellite zenith angles by vegetation subformation using boxplots, which indicate both the spread and median of the distributions. This comparison can help identify whether the viewing geometry in the compositing algorithm is being systematically affected by the reflectance properties of the land-cover type. The spatial autocorrelation of satellite zenith angles in the composites was compared as the third step. Higher autocorrelation would indicate that the composite was more spatially coherent in its viewing geometry. In other words, high spatial autocorrelation means that neighboring pixels values were derived from similar spatial resolution and atmospheric conditions than low autocorrelation does. Moran's I was used as the test statistic. Moran's spatial autocorrelation statistic is calculated only for the four neighboring cells, i.e., a lag of one.

Results

Viewing Geometry of the 1990 Time Series Composites

The distribution of satellite zenith angle averaged over the 19 biweekly compositing periods appears to be highly biased in the westward looking or forward scattering direction (Figure 2). The mean satellite zenith angle for the 1990 California data was +26°. Very few pixels averaged less than 0° (i.e., eastward looking). This may be expected simply because of the geometry of target-sensor-receiving station in South Dakota. That is, California may be at the furthest limits of acquisition from the receiving station, making eastward looking views less likely to be obtained. Eidenshink (1992) reported that approximately 20 daily images or passes were processed in each composite. In examining the daily images for composite period #15, there were 15 files for the 14 days. Because California was only partially imaged on some of the passes, most pixels in California were covered by only eight passes out of the 15.

The satellite zenith angle varied as a function of vegetation subformation. Water, barren land, and grassland, as mapped by CALVEG, tended to be even more extremely off-nadir than the average. Desert scrub and desert hardwoods tended to be viewed closer to nadir than the mean angle. The scaling of NDVI in the compositing process should set nonvegetated surfaces to 100 or slightly less. Water and bare classes, however, had maximum NDVI values over 120 for their medians. Most of the vegetation subformations had differences in angles at the 5 percent significance level.

Our hypothesis for why water and barren types would be viewed at extremely high forescattering angles relates to the issue of spatial resolution. Because these two types have no vegetation cover, their NDVI value should be minimal when viewed at nadir. When viewed off-nadir, particularly to the west, the contribution of surrounding cover types artificially adds to the NDVI signal, and thus this view would be selected over a more accurate nadir view by the MVC algorithm. Consequently, water and barren tended to have higher observed NDVI than desert types, despite their lack of vegetation. An interesting example can be seen at Mono Lake, with Paoha Island in the center (Figure 3). Most of the lake pixels in the composites were high angle views towards the west, incorporating the low vegetation signal of the surrounding grass and scrub cover. The sparsely vegetated island tended to be viewed at close to nadir in the composites, however, to minimize the reduction in NDVI if water were included. As a result, this 7-km^2 island stands out clearly in the zenith angle image. Similarly, bare peaks in the Sierra Nevada show strikingly in this image. In fact, there is remarkable correspondence of map units of subformation types with patterns in the satellite zenith angle image (Figure 3). The dark areas in this figure tend to be lower elevation conifer forests. The lighter band along the western edge of the Central Valley, beginning in the upper left corner, is a narrow band of annual

grassland. Correspondence of the boundaries of the vegetation subformations with changes in zenith angle in this figure is even more striking than the statistical results by class. In the stratified classes, regions of the same vegetation subformation with quite different zenith angle properties tended to cancel each other out. For instance, some grasslands had large zenith angles while other grass pixels were at lower angles, but this figure illustrates that locally, the correspondence of angle with type is quite high. We hypothesize that the large westward zenith angle averages the signal from the densely vegetated crop lands just to the east with the senescent grasslands during the summer season to maximize the observed NDVI. The grassland belt on the east side of the Valley appears somewhat darker, indicating different viewing effects operating within the same cover type in a different geographic circumstance. The texture of the zenith angle image also added to the visual impact of the figure, such as the more heterogeneous appearance of cropland in the Central Valley compared to the smoother looking grassland and oak woodland surrounding it.

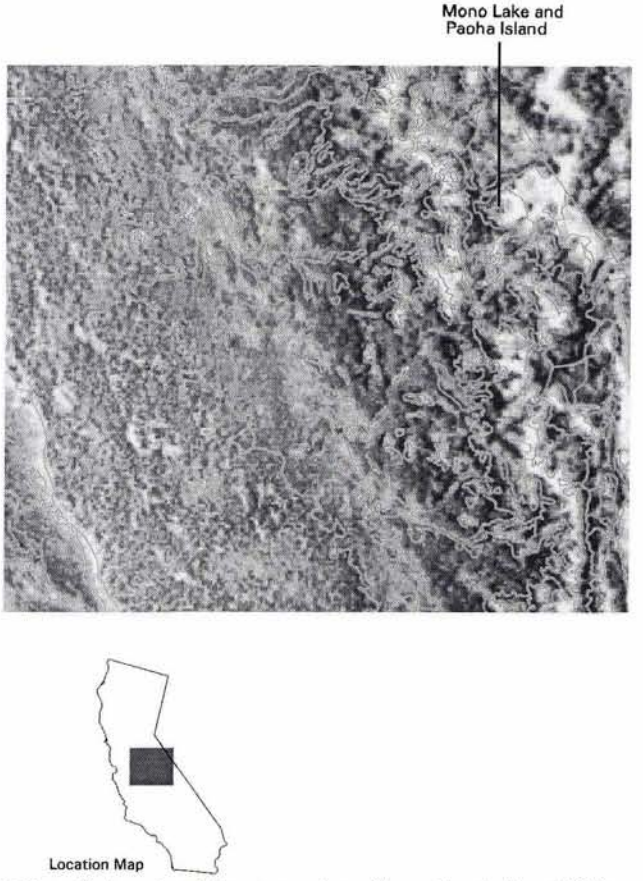

Figure 3. Image of the sum of zenith angles in the 1990 biweekly NDVI composites for a portion of central California. The brighter values indicate pixels with a large off-nadir, westward looking scan angle, while dark values are consistently close to nadir views. The white and black lines are the vegetation subformation types derived from the CALVEG map.

Comparison of Compositing Strategies

A visual comparison of the three alternative composites gave a qualitative assessment. The MVC composite generally looked the least crisp (see Figure 4a for a subimage covering the same extent as Figure 3). Features such as water bodies were less distinct, and the overall impression was more blurry. The MaT composite was sharper than MVC, particularly in the agricultural areas along the left edge of Figure 4b. However, some water bodies (e.g., Mono Lake) were still indistinct. Also notice the smoke plume from a large fire in Yosemite National Park that is trailing northward in the top center of the image. Evidently, the smoke appeared warmer than the ground below. The MVC composite only partially shows this plume. The MOC composite (Figure 4c) was similar in appearance to MaT in that it was sharper than MVC. The smoke plume is still evident in this composite as well, but the shoreline of Mono Lake is more accurately defined.

For a more quantitative measure of sharpness, we compared Moran's I for the three NDVI composites. MVC had the highest spatial autocorrelation at 0.97, while MaT had 0.95 and MOC had 0.94. Although the differences were quite small, the higher value for MVC suggests greater averaging of pixel values from spatial blurring than the other two composites.

The difference in distribution of satellite zenith angles in the three composites was quite striking (Figures 5a to 5c). The MVC composite was based on pixels spread over a wide range of satellite zenith angles (mean of $+17.1°$ and standard deviation of 24.6°), with a peak near nadir but a significant secondary peak above $+40°$. The MaT composite was also distributed around nadir but with a shift toward backscatter views (mean angle of 0.5° and standard deviation of 22.5°). There was also a cluster of pixels at high forescatter views. The MOC composite, on the other hand, was almost entirely derived from satellite zenith angles between $-20°$ and $+15°$, again with a slight shift toward backscatter views (mean of $-2.6°$ and standard deviation of 9.0°). In general, it is clear that the MVC algorithm did not select higher forescatter views simply because closer-to-nadir views were not available.

Figures 6a to 6c depict the effect of land-cover type on the viewing geometry of the three compositing algorithms. The MVC composite (Figure 6a) generally had a much wider spread of values for each class and higher median values than the other two. Water and desert classes, in particular, had much greater medians than the more densely vegetated classes. Some other sparse cover types, such as sagebrush and subalpine conifer, had median angles slightly to the east of nadir although their spread was fairly wide. Only the mixed conifer and hardwood types had relatively compact angle distributions near nadir.

Angle distributions by cover type for the MaT algorithm were generally more compact than with MVC, and medians tended to be closer to nadir (Figure 6b). Water again showed a wide spread of angles but the median was much closer to nadir. Only the mixed conifer type developed a wider angle distribution than occurred with MVC. Cihlar *et al.* (1994) noticed that the maximum-apparent-temperature composite produced a bimodal distribution of angles for coniferous forest in Canada. This accounts for the wide boxplot we observe here as well, particularly where the conifer forests of the northwest corner of California had cloud cover on several days of the compositing period. This region was composited with extremely high satellite zenith angles to avoid the clouds.

The most compact angle distributions for all cover types was found with the MOC algorithm (Figure 6c). Median angles were within 10° of nadir for all types. The wide angle distribution for mixed conifer in the MaT composite was reduced considerably by the addition of a weight for angle in the compositing algorithm. Pixels acquired nearer nadir were found in the northwest region that were close to maximum apparent temperature. This geographic region therefore looks sharper in the MOC than in the MaT composite. The most ex-

(a)

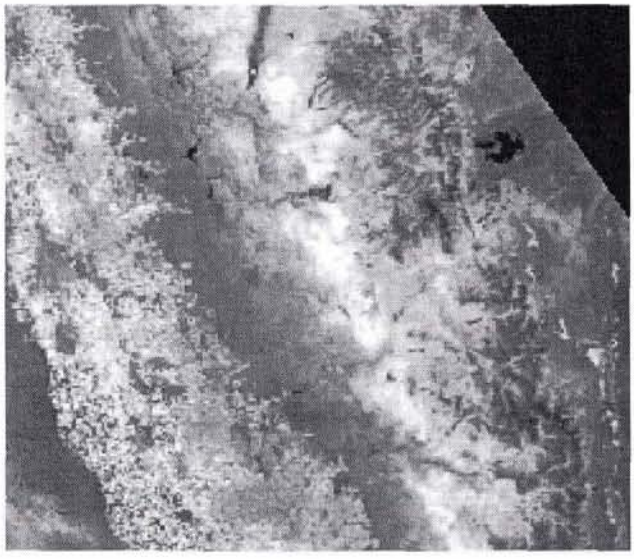

(b)

(c)

Figure 4. Composite NDVI images from the three algorithms for the 14-27 September 1990 period. (a) The Maximum-Value Composite (MVC). (b) The Maximum-Apparent-Temperature Composite (MAT). (c) The Multiple-Objective Composite (MOC). The weights on NDVI, temperature (T), and satellite zenith angle (Z) for MVC: NDVI = 1.0, T = 0.0, Z = 0.0; MAT: NDVI = 0.0, T = 1.0, Z = 0.0; MOC: NDVI = 0.0, T = 1.0, Z = 0.1.

treme backscatter viewing angles occurred for the least densely vegetated types, including barren, herbaceous, sagebrush, and desert scrub, which also had higher backscatter in MAT as well. This may be a result of the reduction in the visibility of plant shadows in the backscatter direction, which would create higher apparent temperatures than forescatter views with greater shadowing.

The Moran's I for satellite zenith angle for MVC was 0.62, for MAT was 0.83, and for MOC was 0.84. Values close to 0 indicate viewing geometry that was not spatially autocorrelated. Therefore, MAT and MOC did a better job of selecting pixels from the same date and viewing geometry as their neighbors.

Discussion and Conclusions

The maximum NDVI algorithm used for generating the dataset of biweekly composites on which the 1990 prototype land-cover database is based tends to select off-nadir viewing angles. On the west coast, this bias is in the forescatter, or westward-looking, direction. Over the 19 biweekly composites, the mean satellite zenith angle for pixels in a California subimage was 26° in the forescatter direction. This finding corroborates findings of Cihlar *et al.* (1994) and Moody and Strahler (1994) for single composite periods in central Canada and the San Francisco Bay Area. Studies on the east coast, however, showed strong bias towards backscatter views (Allen *et al.*, 1994; Moody and Strahler, 1994). Those authors speculated that this effect was related to the lack of forward scatter views at the eastern limit of the receiving range from EDC. Because the work of Deering and Eck (1987) showed, however, that for some land surfaces, NDVI is lowest in the backscatter direction, it is unclear why the MVC algorithm would not pick near nadir views in the absence of those from the forward-scatter direction.

This satellite zenith angle bias caused by the MVC algorithm impacts the accuracy and utility of the NDVI time series in two potential ways. First, the spatial resolution in the composites will be inconsistent. Goward *et al.* (1991) claim that the IFOV becomes significantly distorted at a satellite zenith angle of 30°, which is similar to the average angle of the composite data for California. Not only does this create an uneven sharpness to the image data, it also means that the

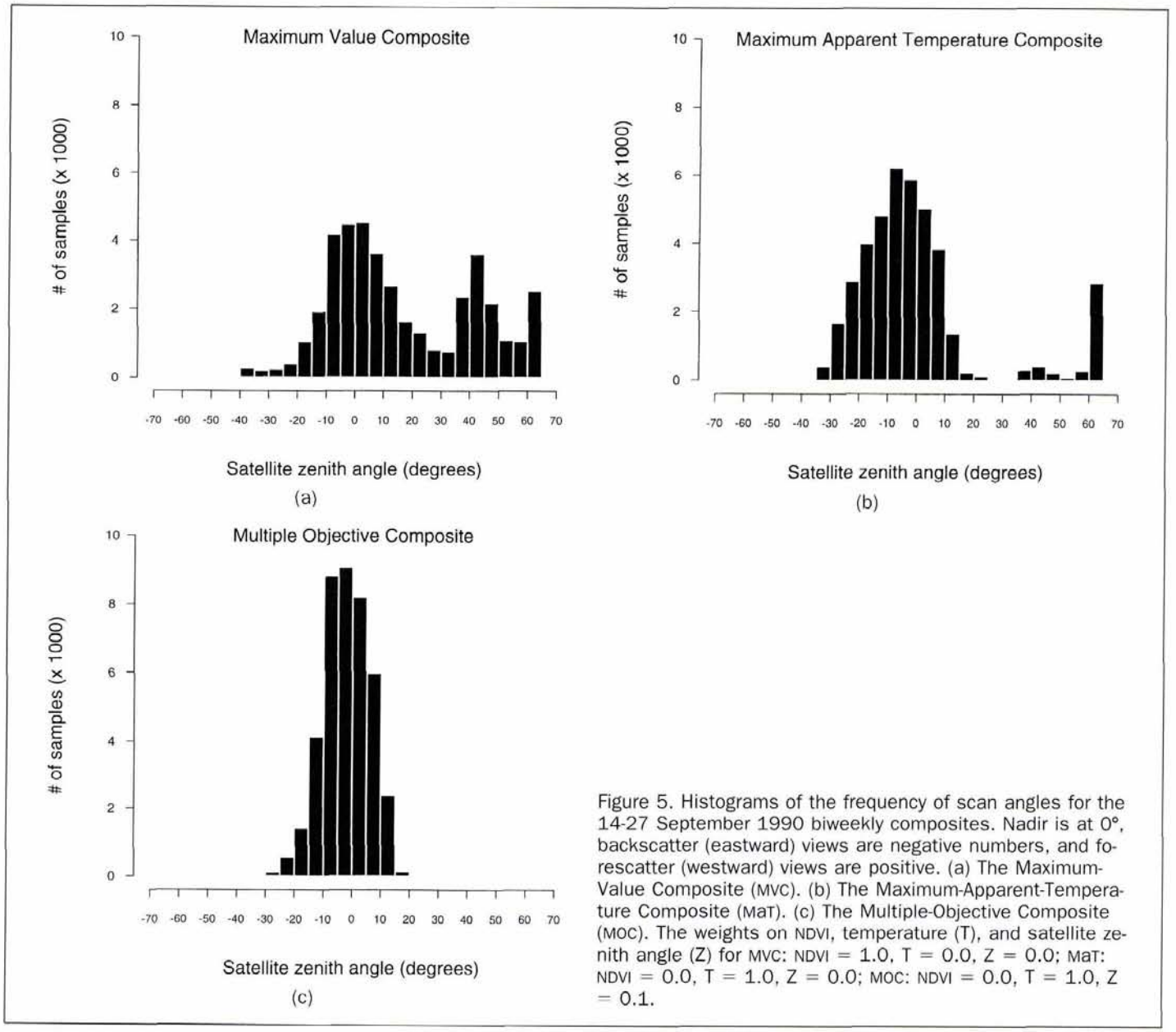

Figure 5. Histograms of the frequency of scan angles for the 14-27 September 1990 biweekly composites. Nadir is at 0°, backscatter (eastward) views are negative numbers, and forescatter (westward) views are positive. (a) The Maximum-Value Composite (MVC). (b) The Maximum-Apparent-Temperature Composite (MAT). (c) The Multiple-Objective Composite (MOC). The weights on NDVI, temperature (T), and satellite zenith angle (Z) for MVC: NDVI = 1.0, T = 0.0, Z = 0.0; MAT: NDVI = 0.0, T = 1.0, Z = 0.0; MOC: NDVI = 0.0, T = 1.0, Z = 0.1.

footprint on the ground integrates signal from outside the image pixel. We found this to be particularly common for areas of extremely low NDVI values such as water and bare rock, where increasing the footprint size artificially enhances the apparent NDVI. In addition, NDVI may increase in off-nadir views because the effects of the bidirectional reflectance function (e.g., scattering, shadowing, and projected canopy cover) all tend to increase the near-IR signal and decrease the red response. Hence, the NDVI ratio is again dependent in part on the look angle chosen, although the degree of dependence varies by surface cover.

Incorporating more than one objective in the compositing process produced time-series data with better viewing properties in this case study than the MVC algorithm with its sole objective of maximizing NDVI or the MAT algorithm which maximizes apparent temperature. The September period is late in the summer dry season in California, but still contained extensive cloud cover in several of the daily images. All three algorithms appeared to remove most clouds, although MOC did so with satellite zenith angles more closely clustered about nadir than the others, particularly in the northwest forested region and over water.

The comparison of alternative compositing algorithms in this study was limited to one 14-day period in a single study area and thus makes generalization difficult. California's geographic position at the extreme western limit of range from the EDC ground receiving station precludes the availability of some eastward viewing opportunities. Located in the northern hemisphere means that California is imaged close to the principal plane of the sun, which accentuates anisotropic effects of both atmosphere and surface. Thus, the study is not fully representative of all regions of the country or the world. Consequently, the set of weights we selected for the MOC algorithm tested here may well not be appropriate for general use. Nevertheless, the multiple-objective approach of weighting greenness, temperature, and viewing angle in compositing can be useful in discovering their relative importance over a range of circumstances. We have found that the weighting scheme appears to work well over a larger geographic region, such as the Great Basin, using 1990 data from

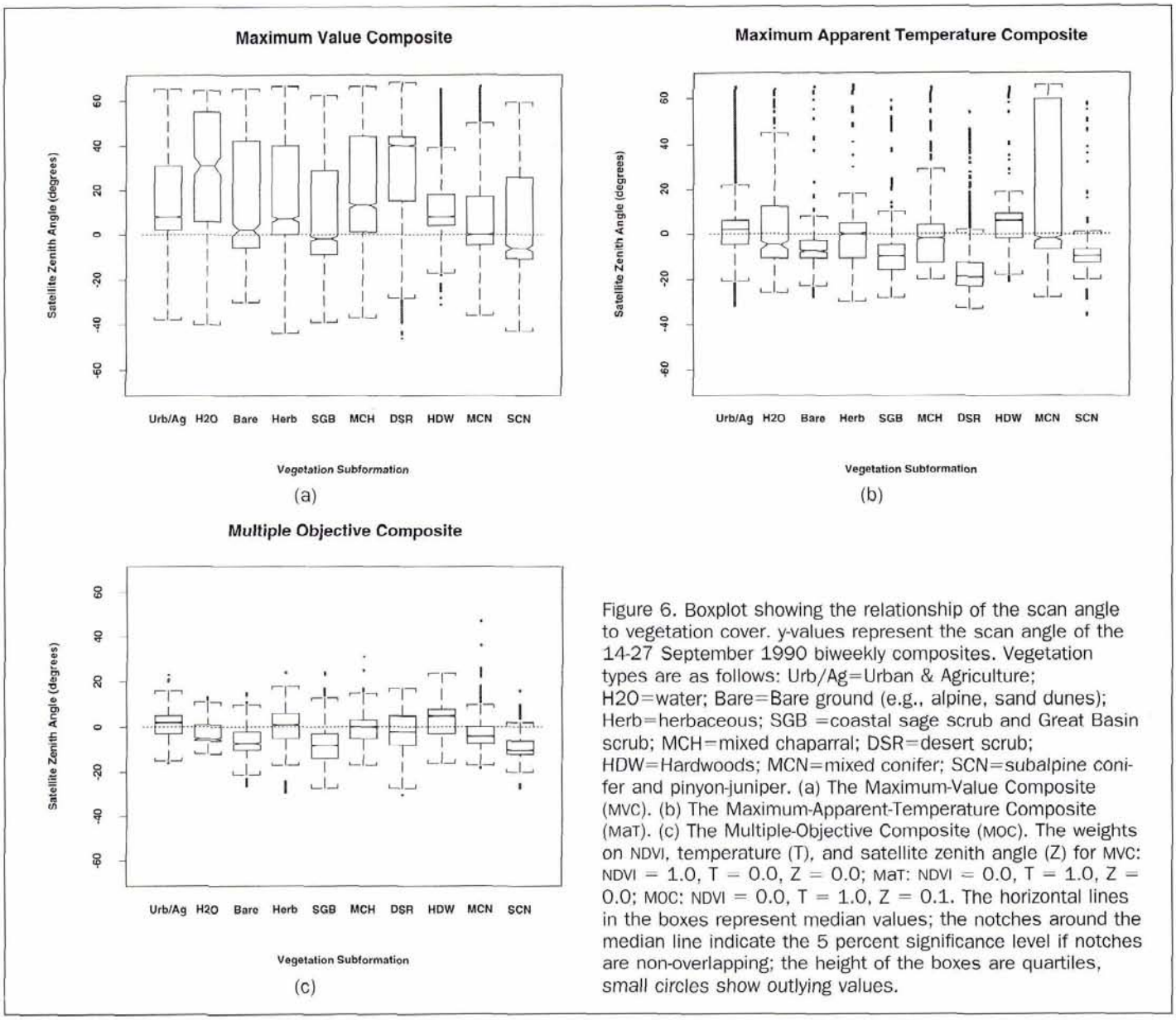

Figure 6. Boxplot showing the relationship of the scan angle to vegetation cover. y-values represent the scan angle of the 14-27 September 1990 biweekly composites. Vegetation types are as follows: Urb/Ag=Urban & Agriculture; H2O=water; Bare=Bare ground (e.g., alpine, sand dunes); Herb=herbaceous; SGB =coastal sage scrub and Great Basin scrub; MCH=mixed chaparral; DSR=desert scrub; HDW=Hardwoods; MCN=mixed conifer; SCN=subalpine conifer and pinyon-juniper. (a) The Maximum-Value Composite (MVC). (b) The Maximum-Apparent-Temperature Composite (MAT). (c) The Multiple-Objective Composite (MOC). The weights on NDVI, temperature (T), and satellite zenith angle (Z) for MVC: NDVI = 1.0, T = 0.0, Z = 0.0; MAT: NDVI = 0.0, T = 1.0, Z = 0.0; MOC: NDVI = 0.0, T = 1.0, Z = 0.1. The horizontal lines in the boxes represent median values; the notches around the median line indicate the 5 percent significance level if notches are non-overlapping; the height of the boxes are quartiles, small circles show outlying values.

several composite periods throughout the growing season. Similarly, it has been successful using recent AVHRR data acquired in Santa Barbara on the Pacific Coast where the full range of viewing angles are available for testing.

MOC is a relatively straightforward, empirical method for exploratory analysis. It differs from the multiple-objective strategies described in Cihlar *et al.* (1994) which operate in two steps. First, all pixels with NDVI values within an empirically set threshold of the maximum value were run through a second step, picking either for minimum scan angle or maximum apparent temperature (depending on the algorithm).

Some problems remain in the use of the selected weights in our study for specific land-cover situations. Snow cover appears cooler than clouds, and, therefore, the algorithm would tend to select cloud pixels over snowpack. The smoke plume from a wildfire in the September images (Figures 4b and 4c) appears warmer than the underlying ground surface; thus, the pixels with smoke were selected over pixels without smoke, even when an angle weight was included. The MAT algorithm likewise has difficulty with snow cover and fire, which limits its utility for global applications. The MVC algorithm generally picked smoke-free data because they have higher NDVI values than does smoke, although some trace of the plume is visible even in Figure 4a. Additional study is needed to account for these unusual circumstances. One advantage of the MOC approach is that the weights for different criteria can be adjusted to accommodate the needs of the analyst, whereas the MVC method is limited to a single criterion with little flexibility. Although the Land Cover Working Group of the International Geosphere-Biosphere Programme Data and Information System is developing global land-cover datasets based on the MVC algorithm (Eidenshink and Faundeen, 1994), preliminary analysis indicates a similar viewing bias of the entire North American dataset averaged over a full year (Yang *et al.*, 1996). We recommend that alternative methods such as MOC be tested further in other regions and seasons.

Acknowledgments

Funding for this study was provided by the U. S. Environmental Protection Agency as part of the federal Biodiversity

Research Consortium, and by the IBM Environmental Research Program. We thank Tom Loveland of the USGS EROS Data Center for all AVHRR data and related products. Brian Biggs and Jason Simpson provided image processing support. We greatly appreciate the thorough comments of the three reviewers. Although the research described in this article has been partially supported by the U.S. Environmental Protection Agency through the Advanced Remote Sensing and Geographic Information System Research Cooperative Agreement # CR-820467-01-1 to Dr. Jack Estes, it has not been subjected to Agency review and therefore does not necessarily reflect the views of the Agency. No official endorsement should be inferred.

References

Allen, T.R., T.J. Bara, and S.J. Walsh, 1994. Observed biases in the Conterminous U.S. AVHRR Satellite Data Set: A North Carolina case study, *Geocarto International*, 9(2):52–62.

Cihlar, J., D. Manak, and M.D-Iorio, 1994. An evaluation of compositing algorithms for AVHRR data over land, *IEEE Transactions on Geoscience and Remote Sensing*, 32(2):427–437.

Deering, D.W., and T.F. Eck, 1987. Atmospheric optical depth effects on angular anisotropy of plant canopy reflectance, *International Journal of Remote Sensing*, 8(6):893–916.

Eidenshink, J.C., 1992. The 1990 Conterminous U.S. AVHRR data set, *Photogrammetric Engineering & Remote Sensing*, 58(6):809–813.

Eidenshink, J.C., and J.L. Faundeen, 1994. The 1 km AVHRR global land data set: First stages in implementation, *International Journal of Remote Sensing*, 15(17):3443–3462.

Goward, S.N., B. Markham, D.G. Dye, W. Dulaney, and J. Yang, 1991. Normalized difference vegetation index measurements from the Advanced Very High Resolution Radiometer, *Remote Sensing of Environment*, 35(2):257–277.

Gutman, G.G., 1991. Vegetation indices from AVHRR: An update and future prospects, *Remote Sensing of Environment*, 35(2–3): 121–136.

Holben, B.N., 1986. Characteristics of maximum-value composite images from temporal AVHRR data, *International Journal of Remote Sensing*, 7(11):1417–1437.

Holben, B.N., D.S. Kimes, and R.S. Fraser, 1986. Directional reflectance response in AVHRR red and near IR bands for three cover types and varying atmospheric conditions, *Remote Sensing of Environment*, 19(3):213–236.

Kasischke E.S., N.H.F. French, P. Harrell, N.L. Christensen, Jr., S.L. Ustin, and D. Barry, 1993. Monitoring of wildfires in boreal forests using large area AVHRR NDVI composite image data, *Remote Sensing of Environment*, 45(1):61–71.

Kremer, R.G., and S.W. Running, 1993. Community type differentiation using NOAA/AVHRR data within a sagebrush-steppe ecosystem, *Remote Sensing of Environment*, 46(3):311–318.

Loveland, T.R., J. Merchant, D.O. Ohlen, and J. Brown, 1991. Development of a land cover characteristics data base for the conterminous U.S., *Photogrammetric Engineering & Remote Sensing*, 57(11):1453–1463.

Matyas, W.J., and I. Parker, 1980. *CALVEG; A Classification of Californian Vegetation*, Regional Ecology Group, U.S. Forest Service, San Francisco.

Moody, A., and A.H. Strahler, 1994. Characteristics of composited AVHRR data and problems in their classification, *International Journal of Remote Sensing*, 15(17):3473–3491.

Paruelo, J.M., and W.K. Lauenroth, 1995. Regional patterns of normalized difference vegetation index in North American shrublands and grasslands, *Ecology*, 76(6):1888–1898.

Reed, B.C., J.F. Brown, D. VanderZee, T.R. Loveland, J.W. Merchant, and D.O. Ohlen, 1994. Measuring phenological variability from satellite imagery, *Journal of Vegetation Science*, 5(5):703–714.

Statistical Sciences, Inc., 1991. *S-PLUS User's Manual*, Seattle, Washington.

Townshend, J.R.G., C.O. Justice, D. Skole, J.-P. Malingreau, J. Cihlar, P. Teillet, F. Sadowski, and S. Ruttenberg, 1994. The 1 km resolution global data set: Needs of the International Geosphere Biosphere Programme, *International Journal of Remote Sensing*, 15(17):3417–3441.

U.S.G.S., 1991. *Conterminous U.S. AVHRR 1990 Biweekly Composites* (CD-ROM), National Mapping Division, EROS Data Center, Sioux Falls, South Dakota.

Viovy, N., O. Arino, and A.S. Belward, 1992. The best index slope extraction (BISE): A method for reducing noise in NDVI time-series, *International Journal of Remote Sensing*, 13(8):1585–1590.

Wade, G., R. Mueller, P. Cook, and P. Doraiswamy, 1994. AVHRR map products for crop condition assessment: A geographic information systems approach, *Photogrammetric Engineering & Remote Sensing*, 60(9):1145–1150.

Walker, R.E., D.M. Stoms, J.E. Estes, and K.D. Cayocca, 1992. Improved modeling of biological diversity with multitemporal vegetation index data, *Technical Papers of the 1992 Annual Meeting of ASPRS/ACSM*, Albuquerque, New Mexico, 3-8 March, pp. 562–571.

Yang, L., Z.-L. Zhu, J.A. Izaurralde, and J.W. Merchant, 1996. Evaluation of North and South America AVHRR 1-km data for global environmental modeling, *Proceedings of the Third International Conference/Workshop on Integrating GIS and Environmental Modeling*, National Center for Geographic Information and Analysis, Santa Barbara, California (CD and WWW).

(Received 20 July 1995; revised and accepted 1 November 1996)